

Manuscript Number: MRB-11-510R2

Title: Synthesis and characterization of TiO<sub>2</sub> powders by electrospray pyrolysis method

Article Type: Research Paper

Keywords: ceramics; oxides; chemical synthesis; vapor deposition

Corresponding Author: Prof. Yoshikazu Suzuki, Ph.D.

Corresponding Author's Institution: University of Tsukuba

First Author: Yoshihiro Terada, MS

Order of Authors: Yoshihiro Terada, MS; Yoshikazu Suzuki, Ph.D.; Susumu Tohno, Ph.D.

Abstract: Electrospray pyrolysis, i.e. combination of electrospray and in-flight thermal treatment, has attracted much attention as a preparation method of functional ceramic particles. In this paper, we report the processing detail of spherical TiO<sub>2</sub> nano- and microparticles by the electrospray pyrolysis method as well as their photocatalytic activity for hydrogen evolution. Titanium(IV) bis (ammonium lactato) dihydroxide aqueous solutions (TALH aq. 0.2-20 wt%) were injected into a capillary nozzle by a syringe pump (0.15-0.59 mL/min), and were electrosprayed by using DC 4 kV voltage, followed by the pyrolysis at 300-500°C. Spherical TiO<sub>2</sub> nano- and microparticles were successfully obtained. Effects of precursor-liquid concentration, liquid flow-rate, and pyrolysis temperature on the particle size, microstructure and functions were discussed.

## Synthesis and characterization of TiO<sub>2</sub> powders by electrospray pyrolysis method

Yoshihiro Terada,<sup>1</sup> Yoshikazu Suzuki,<sup>2\*</sup> and Susumu Tohno<sup>1\*</sup>

<sup>1</sup>Graduate School of Energy Science, Kyoto University, Yoshida Honmachi, Sakyo-Ku, Kyoto 606-8501, Japan

<sup>2</sup> Graduate School of Pure and Applied Sciences, University of Tsukuba, Tsukuba, Ibaraki 305-8573, Japan

### Abstract

Electrospray pyrolysis, *i.e.* combination of electrospray and in-flight thermal treatment, has attracted much attention as a preparation method of functional ceramic particles. In this paper, we report the processing detail of spherical TiO<sub>2</sub> nano- and microparticles by the electrospray pyrolysis method as well as their photocatalytic activity for hydrogen evolution. Titanium(IV) bis (ammonium lactato) dihydroxide aqueous solutions (TALH aq. 0.2-20 wt%) were injected into a capillary nozzle by a syringe pump (0.15-0.59 mL/min), and were electrosprayed by using DC 4 kV voltage, followed by the pyrolysis at 300-500°C. Spherical TiO<sub>2</sub> nano- and microparticles were successfully obtained. Effects of precursor-liquid concentration, liquid flow-rate, and pyrolysis temperature on the particle size, microstructure and functions were discussed.

### Keywords:

ceramics; oxides; chemical synthesis; vapor deposition

### 1. Introduction

Electrospray is a phenomenon generating ultrafine droplets, when a high voltage is applied to the surface of liquid [1,2]. Semispherical liquid at the tip of capillary nozzle receives electrostatic force as well as surface tension and gravity, when the voltage of several kV is applied between a liquid-supplying capillary and a counter electrode. The

---

\*Corresponding authors:

E-mail: [suzuki@ims.tsukuba.ac.jp](mailto:suzuki@ims.tsukuba.ac.jp) (Y. Suzuki)

E-mail: [tohno@energy.kyoto-u.ac.jp](mailto:tohno@energy.kyoto-u.ac.jp) (S. Tohno)

resultant force distorts the liquid into a cone shape, and then, a spray of ultrafine droplets is generated. With controlling the quantity of electricity depending on the liquid supply, continuous and uniform droplets can be obtained. The size of the droplets ranges from nm to mm order, depending on the liquid flow rate, electric conductivity of the liquid, and applied voltage. Due to the repulsive Coulomb forces, relatively good dispersion state can be achieved by the electrospray technique. After the Fenn's innovative works [2], electrospray technique has been widely used for the ion source for mass spectrometry.

Currently, electrospray is also used as a new powder-processing method. In particular, electrospray pyrolysis (*i.e.*, combination of electrospray and in-flight thermal treatment) has attracted much attention as a preparation method of functional ceramic particles, as indicated in Fig. 1 [3]. Lenggono et al. [4-5] reported the synthesis of ZnS nanoparticles by the electrospray pyrolysis method, equipped with  $\alpha$ -ray radioactive source ( $^{241}\text{Am}$ ; 2.22 MBq) for the neutralization of charged droplets. Nakaso et al. [6] prepared non-agglomerated spherical  $\text{SiO}_2$ ,  $\text{TiO}_2$  and  $\text{ZrO}_2$  nanoparticles using electrospray assisted CVD (ES-CVD) method. Kuroda et al. synthesized ZnS nanoparticles by electrospray method with rectangular AC high voltage (instead of conventional DC high voltage) to suppress the particle agglomeration and the deposition to the chamber wall [7]. In previous reports on the electrospray pyrolysis method for nanoparticles processing, much effort has been paid for the particle-size distribution analysis as well as the crystal structure analysis [3]. However, functional properties of synthesized ceramic particles are not widely reported.

We report the processing details of spherical  $\text{TiO}_2$  nano- and microparticles by the electrospray pyrolysis method as well as their photocatalytic activity for hydrogen evolution. At first, droplet size for the electrospray in cone-jet mode was quantitatively characterized by a digital microscope. Second, Scanning Mobility Particle Sizer<sup>TM</sup> (SMPS) was used to determine of the number size distribution of the synthesized aerosol particles by electrospray pyrolysis method. Using these data, optimum conditions to obtain  $\text{TiO}_2$  nano- and microparticles are discussed. And finally, photocatalytic activity for  $\text{H}_2$  evolution was studied for the anatase  $\text{TiO}_2$  powders prepared by the electrospray pyrolysis.

## 2. Experimental Procedure

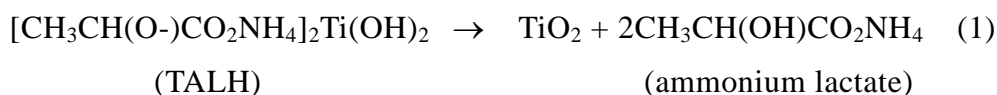
### 2.1 Measurement of droplet size for Electrospray (without pyrolysis)

At first, in order to characterize aerosol properties, electrosprayed droplet size was quantitatively analyzed. 0.2-20 wt% Titanium(IV) bis (ammonium lactato) dihydroxide aqueous solution (TALH aq., diluted from a commercial 50% aqueous solution, Sigma-Aldrich [8,9]) was used as a precursor of TiO<sub>2</sub>. TALH aqueous solutions (0.2, 2.0 and 20 wt%) were injected into a capillary nozzle by a syringe pump (flow rate: 0.15, 0.3 and 0.59 mL/min), and were electrosprayed by using positive DC 4 kV voltage (HSX-10R 1.5, Matsusada Precision Inc.) A stainless steel capillary nozzle, inner diameter: 0.92 mm, outer diameter: 1.28 mm, length: 30 mm (Musashi Engineering Inc.) was used.

Electrosprayed droplets (charged by DC voltage) were collected for 30 s on aluminum foil with opposite charge (using another voltage source, 1 kV). Droplets were fixed by a polymerization method using  $\alpha$ -cyanoacrylate, major component of instantaneous adhesive, developed by our group [10]. Approximately one hundred fixed droplets were observed by using a digital microscope (VHX-100, Keyence. Co) to determine the average diameter of the droplets.

### 2.2 Electrospray-pyrolysis: Synthesis and In-situ Particle-Size Analysis

TiO<sub>2</sub> particles are formed through the pyrolytic reaction (1) of TALH in the droplets:



By using this pyrolytic reaction, spherical TiO<sub>2</sub> nano- and microparticles were formed. Tubular electric furnace with a glass tube reactor (length: 60 cm, diameter: 50 mm, 300-500°C) was used for the pyrolysis. A stream of dry clean air (2L/min) was used as a carrier gas. Resultant TiO<sub>2</sub> particles in carrier gas were diluted by dry air, passed through a diffusion dryer of silica gel, and particle size distribution of the aerosols was measured by a Scanning Mobility Particle Sizer<sup>TM</sup> (SMPS Moel-3034, TSI). SMPS enables to measure particles in the size of 10-500 nm in diameter. (As for larger particles, i.e., > 500 nm, SEM was used as shown later.)

### *2.3 Electrospray-pyrolysis: Powder Production and Characterization*

In order to prepare  $\text{TiO}_2$  powders by electrospray pyrolysis, high-throughput conditions with keeping fine particle sizes are favored. According to preliminary experiments, TALH concentration of 20 wt% and liquid flow rate of 0.15 mL/min were used for the powder processing and its functional analysis.  $\text{TiO}_2$  powders were collected by an electrostatic collector with opposite charge (using voltage source of 1 kV). Other electrospray pyrolysis conditions are the same as above.

Microstructure of the  $\text{TiO}_2$  powders was observed by SEM (JSM-6500F, JEOL). The constituent phases of the powder were analyzed by XRD (Cu-K $\alpha$ , 40 kV and 40 mA, MultiFlex, Rigaku). The photocatalytic  $\text{H}_2$  evolution (water splitting) was carried out in a closed gas-circulation in an inner irradiation-type photoreactor made of Pyrex glass as described in previous works [10-14].  $\text{TiO}_2$  powders (1 g) prepared by electrospray pyrolysis (pyrolysis temperatures: 300, 400 and 500°C) were suspended in aqueous ethanol solution (720 mL distilled  $\text{H}_2\text{O}$  + 80 mL ethanol) by using a magnetic stirrer. A high-pressure Hg lamp (Ushio, Japan; UM-452, 450 W) was utilized as the UV light source. The mixture was deaerated by purging with Ar gas stream. To maintain the reaction temperature, cooling water was circulated through a cylindrical Pyrex jacket located around the light source. The evolved gasses were periodically analyzed by an on-line gas chromatograph (Shimadzu GC-8A, Molecular sieve 5A, TCD, Ar Carrier) until the reaction time reached 3 h. A commercial  $\text{TiO}_2$  powder (P-25, Degussa/Nippon Aerosil Co., Ltd., mean primary particle size of 21 nm) was used as a reference material.

## **3. Results and Discussion**

### *3.1 Droplet size: effects of precursor concentration and liquid flow rate*

Figure 2 shows the effects of precursor concentration on the droplet size. Figs. 2(a) -(c) demonstrate digital optical micrographs of electrosprayed droplets fixed by cyanoacrylate vapor, for TALH concentrations of 0.2%, 2%, and 20%, respectively under 0.3mL/min of liquid flow rate. Fig. 2(d) summarizes the average droplet diameter vs. concentration for different flow rates. Fig. 2(d) shows a definite positive correlation between the droplet size and the precursor concentration.

Figure 3 shows the effect of the liquid flow rate on the droplet size. Figs. 3(a) -(c)

demonstrate digital optical micrographs of electrosprayed droplets, where the TALH concentration was 2% and liquid flow rates were (a) 0.15, (b) 0.30, and (c) 0.59 mL/min, respectively. Fig. 3(d) depicts the average droplet diameter vs. flow rate for different concentrations. Fig. 3(d) demonstrates that the droplet size also increased with increasing the flow rate.

Rosell-Llompart and Fernández de la Mora [15] reported that the relationship between droplet size and operating conditions of the electrospray are expressed as a following equation (Scaling law):

$$D_d = G(\varepsilon)(Q\varepsilon_0 / K)^{\frac{1}{3}} \quad (2)$$

where  $D_d$  is droplet diameter,  $Q$  is liquid volume flow rate,  $\varepsilon$  is dielectric constant of liquid,  $\varepsilon_0$  is the electrical permittivity of vacuum,  $K$  is electrical conductivity of the liquid.  $G$  is a constant, mainly depending on  $\varepsilon$  [15-17]. From Eq. 2, effects of the precursor concentration on the droplet size (Fig. 2) can be attributable to the change of  $K$ . With increasing the precursor concentration, electrical conductivity of the liquid,  $K$ , decreases, resulting in the increase of  $D_d$ . Effects of the flow rate (Fig. 3) can be directly explained from Eq. 2. Although the general dependence of droplet diameter on the concentration and flow rate agreed qualitatively with that determined by the scaling law, there was discrepancy in scaling factor between measured data and the scaling law of Eq. 2. This is because the parameter  $G$  depends not only on  $\varepsilon$  but also the viscosity ( $\mu$ ) and the surface tension ( $\gamma$ ) of liquid [15-17]. Actually, when the concentration was more than 20%, high viscosity of the liquid resulted in plugging up the nozzle.

### 3.2 Particle size of $\text{TiO}_2$ : effects of the concentration and flow rate of liquid

Figs. 4(a)-(c) show the effect of the precursor-liquid concentration (0.2, 2 and 20%) on the  $\text{TiO}_2$  particle size; pyrolysis temperatures were (a) 300°C, (b) 400°C and (c) 500°C. Precursor-liquid flow rate was fixed as 0.15 mL/min.  $\text{TiO}_2$  particle size (of < 500 nm) was measured by SMPS. As can be seen from these figures, the particle size increased with increasing the concentration. This result can be easily explained by the volume fraction of water in droplets as well as the droplet size (as explained above). When the concentration of the liquid was higher, less water vaporized during the pyrolysis. In addition, droplets themselves were somewhat larger when the

concentration was higher (Fig. 2).

Suppose the solid particles after pyrolysis have spherical shape, the relationship between solid particle size and liquid droplet size can be expressed as follows [16]:

$$d_p^3 = (MD_p^3 C_s) / (1000\rho) \quad (3)$$

where  $d_p$  is the size of a solid particle,  $M$  is molecular weight of  $\text{TiO}_2$ ,  $D_d$  is the size of a liquid droplet,  $C_s$  is the molar concentration of TALH, and  $\rho$  is the density of the solid particle. Then, solid particle size can be calculated using  $C_s$  and the measured droplet diameter shown in Fig. 3(d). Fig. 4(d) shows measured and calculated particle sizes vs. concentrations. Mode diameter was used to represent the measured diameter. The dependence of the particle size for the pyrolysis at 400°C was similar to those of calculated from Eq. 3. It may suggest that the water in droplets was well-vaporized at 400°C without significant grain growth of solid particles. For more detailed analysis, effect of organic component (i.e., ammonium lactate) and un-measured large particles (> 500 nm) should be considered.

Figs. 5 (a)-(c) show the effect of the precursor-liquid flow rate (0.15, 0.30 and 0.59 mL/min) on the  $\text{TiO}_2$  particle size; pyrolysis temperatures were (a) 300°C, (b) 400°C and (c) 500°C. Precursor-liquid concentration was fixed as 0.2 %. As can be seen from these figures, the particle size increased with increasing the flow rate, which is attributed to the increased droplet size (Fig. 3). Fig. 5 (d) shows measured and calculated (from Eq.3, scaling law) particle sizes vs. flow rates. Although the slopes of the regression lines for measured values are similar to that of the calculated values, measured diameters (for obtained  $\text{TiO}_2$  particles) were much larger than calculated ones. This difference can be attributable to the (1) effect of residual organic component (i.e., insufficient thermal decomposition of the ammonium lactate) , (2) coalescence of the droplets, and (3) coagulation of the particles.

### 3.3 Microstructure of the $\text{TiO}_2$ powders by electrospray pyrolysis

$\text{TiO}_2$  powders prepared by electrospray pyrolysis (at 500°C) were collected on the aluminum plate and were observed by SEM (Fig. 6). The flow rate and concentration of the precursor liquid were (a) 0.15 mL/min and 0.2%, (b) 0.59 mL/min and 0.2%, and (c) 0.15 mL/min and 20%, respectively. From the SEM observation, particle size

distributions of each condition were (a) ca. 70-300 nm, (b) ca. 300-2000 nm, and ca. 500-4000 nm. Larger particles were formed with increasing flow rate (Figs. 6(a) and (b)) and with an increase of concentration (Figs. 6(a) and (c)). These tendencies are the same as the SMPS measurement in the previous section. In Fig. 6(a), the size of the particles observed by SEM was in good agreement with that by SMPS. However, in Figs. 6(b) and 6(c), larger particles of several  $\mu\text{m}$  were frequently observed by SEM. (Particles with aerodynamic diameter of larger than 500 nm were removed by the impactor installed at the inlet of SMPS.)

### 3.4 XRD analysis and photocatalytic activity of the $\text{TiO}_2$ powders

Figs. 7(a)-(c) show the appearances of  $\text{TiO}_2$  powders prepared by electrospray pyrolysis method (flow rate: 0.15 mL/min and concentration of 20%) at (a) 300°C, (b) 400°C and (c) 500°C, and Figs. 7(d) shows their XRD patterns. Colored powders (orange, brown and gray, respectively) were obtained **presumably** due to the residual organic impurities. XRD patterns of these powders mainly corresponded to anatase  $\text{TiO}_2$  phase with relatively low crystallinity. Post calcination in an electric furnace at 650°C allowed the formation of white anatase-based  $\text{TiO}_2$  powder with higher crystallinity (Fig. 8). In this case, some (minor) rutile phase was also found in the heat-treated powder. The XRD pattern with additional heat treatment was, as a result, similar to that of P-25 (main anatase + minor rutile phases).

The result (in Fig. 7) demonstrates that  $\text{TiO}_2$  powders produced by our electrospray pyrolysis method contained some residual organic impurities. In some case, these powders with organic impurities show superior functional properties than pure  $\text{TiO}_2$ . Such an example is given as follows.

Figure 9 indicates an example of photocatalytic activity ( $\text{H}_2$  evolution) using the powders in Fig. 7 (i.e., with in-flight heating at 300-500°C but without post heat-treatment). A commercial  $\text{TiO}_2$  powder (P-25) was used as a reference. As can be seen from Fig. 9,  $\text{TiO}_2$  powder prepared by the electrospray pyrolysis at 500°C showed the best performance. This result can be explained by the combination of (i) impurity effect (residual organics acted as sacrificial agent for oxygen), (ii) doping effect (absorbing visible light, potentially by nitrogen or carbon doping) and (iii) reasonable surface area and crystallinity. Post-calcination of the powder at 650°C (as shown in Fig.



8) reduced the photocatalytic activity by almost half, although the co-existence of minor rutile phase is said to have some positive effect for photocatalytic properties (as is P-25). This result supports the above potential reasons of (i)-(iii).

#### 4. Conclusions

We have prepared spherical TiO<sub>2</sub> nano- and microparticles by the electrospray pyrolysis method. Both droplet (by sole electrospray) and particle (by electrospray pyrolysis) size was controllable, and larger particles were produced with increasing precursor-liquid concentration and liquid volume flow rate. Colored powders (orange for 300°C, brown for 400°C and gray for 500°C, respectively) were obtained due to the residual organic impurities. The TiO<sub>2</sub> powder prepared by the electrospray pyrolysis at 500°C exhibited better performance on H<sub>2</sub> evolution, which is a positive aspect to use the electrospray pyrolysis method. Further microstructural control, such as processing of well-controlled hollow spheres [18] and well-controlled primary nanoparticles [19], will be promising to improve the photocatalytic activities.

#### Acknowledgements

The authors wish to thank Prof. Motoaki Adachi and Mr. Syun Kuroda at Osaka Prefecture University for their help to design the electrospray apparatus. A part of this work is supported by Grant-in-Aid for Science Research No. 19685020 (For Young Scientist, Category A), and Global COE Program, MEXT, Japan.

#### References

1. J. Zeleny, Phys. Rev., **3** (1914) 69.
2. J. B. Fenn, M. Mann, C. K. Meng, S. F. Wong, C. M. Whitehouse, Science, **246** (1989) 64.
3. A. Jaworek and A.T. Sobczyk, J. Electrostatics, **66** (2008) 197.
4. I. W. Lenggoro, K. Okuyama, J. Fernandez de la Mora, and N. Tohge, J. Aerosol Sci., **31** (2000) 121.
5. I. W. Lenggoro and K. Okuyama, J. Aerosol Res., **20** (2005) 116.
6. K. Nakaso, B. Han, K. H. Ahn, M. Choi and K. Okuyama, J. Aerosol Sci. **34** (2003) 869.

7. S. Kuroda, N. Yokoyama, T. Kinoshita and M. Adachi, *J. Aerosol Res.*, **23** (2008) 94.
8. H. Möckel, M. Giersig and F. Willig, *J. Mater. Chem.*, **9** (1999) 3051.
9. Y. Suzuki, B. P. Pichon, D. D'Elia, C. Beauger and S. Yoshikawa, *J. Ceram. Soc. Jpn.*, **117** (2009) 381.
10. M. Kasahara, S. Akashi, C.-J. Ma, S. Tohno, *Atmospheric Res.*, **65** (2003) 251.
11. J. Jitputti, S. Pavasupree, Y. Suzuki and S. Yoshikawa, *J. Solid State Chem.*, **180** (2007) 1743.
12. J. Jitputti, S. Pavasupree, Y. Suzuki, and S. Yoshikawa, *Jpn. J. Appl. Phys.*, **47** (2008) 751.
13. J. Jitputti, Y. Suzuki and S. Yoshikawa, *Catal. Comm.*, **9** (2008) 1265.
14. J. Jitputti, T. Ratanavoravipa, S. Chuangchote, S. Pavasupree, Y. Suzuki, and S. Yoshikawa, *Catal. Comm.*, **10** (2009) 378.
15. J. Rosell-Llompart, J. Fernández de la Mora, *J. Aerosol Sci.*, **25** (1994) 1093.
16. I. W. Lenggoro and K. Okuyama, *Proc. Inst. Electrostat. Jpn.*, **21** (1997) 258.
17. I. W. Lenggoro and K. Okuyama, *J. Soc. Powder Technol. Jpn.*, **37** (2000) 753.
18. C. Y. Song, W. J. Yu, B. Zhao, H. L. Zhang, C. J. Tang, K. Sun, X. C. Wu, L. Dong and Y. Chen, *Catal. Comm.*, **10** (2009) 650.
19. A. Chowdhury, A. Kudo, T. Fujita, M. W. Chen and T. Adschiri, *J. Supercritical Fluids*, **58** (2011) 136.

## Figure Captions

**Fig. 1** Synthesis of fine powders by electrospray pyrolysis method [3].

**Fig. 2** Effect of the precursor-liquid concentration on the droplet size; digital optical micrographs of electrosprayed droplets fixed by cyanoacrylate vapor, where the liquid flow rate was 0.30 mL/min and TALH concentrations: (a) 0.2%, (b) 2%, and (c) 20%. (d) Average droplet diameter vs. concentration.

**Fig. 3** Effect of the precursor-liquid flow rate on the droplet size; digital optical micrographs of electrosprayed droplets fixed by cyanoacrylate vapor, where the TALH concentration was 2% and liquid flow rates: (a) 0.15, (b) 0.30, and (c)

0.59 mL/min. (d) Average droplet diameter vs. liquid flow rate.

**Fig. 4** Effect of the precursor-liquid concentration (0.2, 2 and 20%) on the TiO<sub>2</sub> particle size; pyrolysis temperatures were (a) 300°C, (b) 400°C and (c) 500°C. (d) TiO<sub>2</sub> particle diameter vs. concentration. Precursor-liquid flow rate was fixed as 0.15 mL/min.

**Fig. 5** Effect of the precursor-liquid flow rate (0.15, 0.30 and 0.59 mL/min) on the TiO<sub>2</sub> particle size; pyrolysis temperatures were (a) 300°C, (b) 400°C and (c) 500°C. (d) TiO<sub>2</sub> particle diameter vs. liquid flow rate. Precursor-liquid concentration was fixed as 0.2 %.

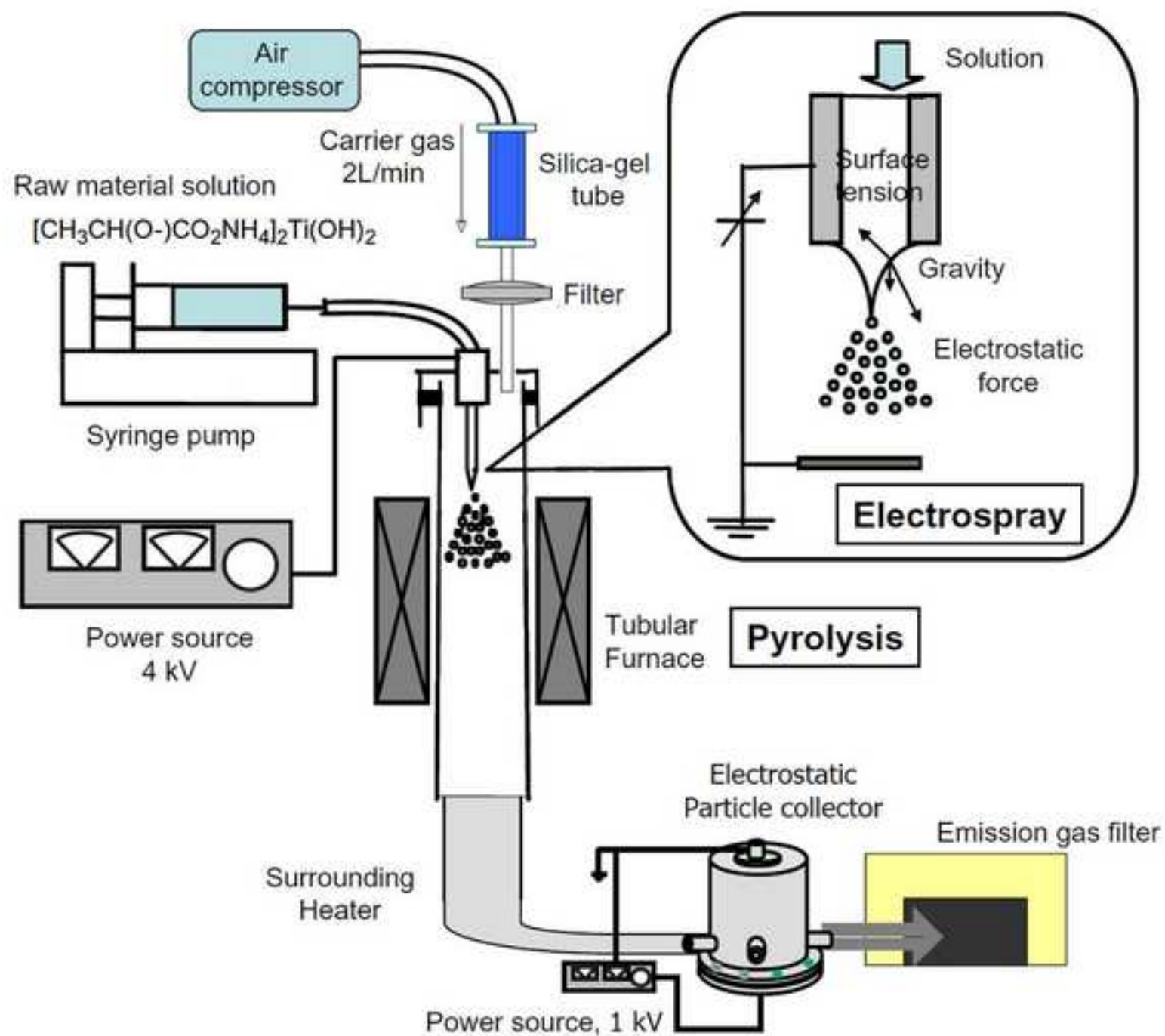
**Fig.6** SEM micrographs of TiO<sub>2</sub> particles prepared by electrospray pyrolysis method. Applied voltage: 4 kV, Carrier gas: 1 L/min, pyrolysis temperature: 500°C. (a) liquid flow rate: 0.15 mL/min and concentration of 0.2%, (b) 0.59 mL/min and 0.2%, and (c) 0.15 mL/min and 20%.

**Fig. 7** TiO<sub>2</sub> powders prepared by electrospray pyrolysis method at different pyrolysis temperatures: (a) 300°C, (b) 400°C and (c) 500°C, (d) XRD patterns (liquid flow rate: 0.15 mL/min and concentration of 20%).

**Fig. 8** XRD pattern for the TiO<sub>2</sub> powder with post calcination at 650°C.

**Fig. 9** Photocatalytic H<sub>2</sub> evolution from water splitting reaction over the TiO<sub>2</sub> powders made by electrospray pyrolysis method (at 300-500°C). A commercial TiO<sub>2</sub> powder (P-25) was also measured under the same conditions as a reference.

**Fig. S1** Schematic illustrations of (a) droplet size measurement system, (b) fixation of droplets [10], (c) electrospray-pyrolysis system for in-flight particle size analysis, and (d) electrospray-pyrolysis system for powder processing. The powder yield was calculated to be ~6% at the electrostatic collector (Fig. S1(d)). To improve the yield, optimization of the reactor is on going.



## \*Highlights

>We report the processing of spherical  $\text{TiO}_2$  particles by the electrospray pyrolysis and their photocatalytic activity.

>Titanium(IV) aqueous solutions were electrosprayed and then pyrolyzed at 300-500°C.

>Spherical  $\text{TiO}_2$  nano- and microparticles were successfully obtained.

>Effects of electrospray pyrolysis conditions on the particle size, microstructure and functions were discussed.

Figure1

[Click here to download high resolution image](#)

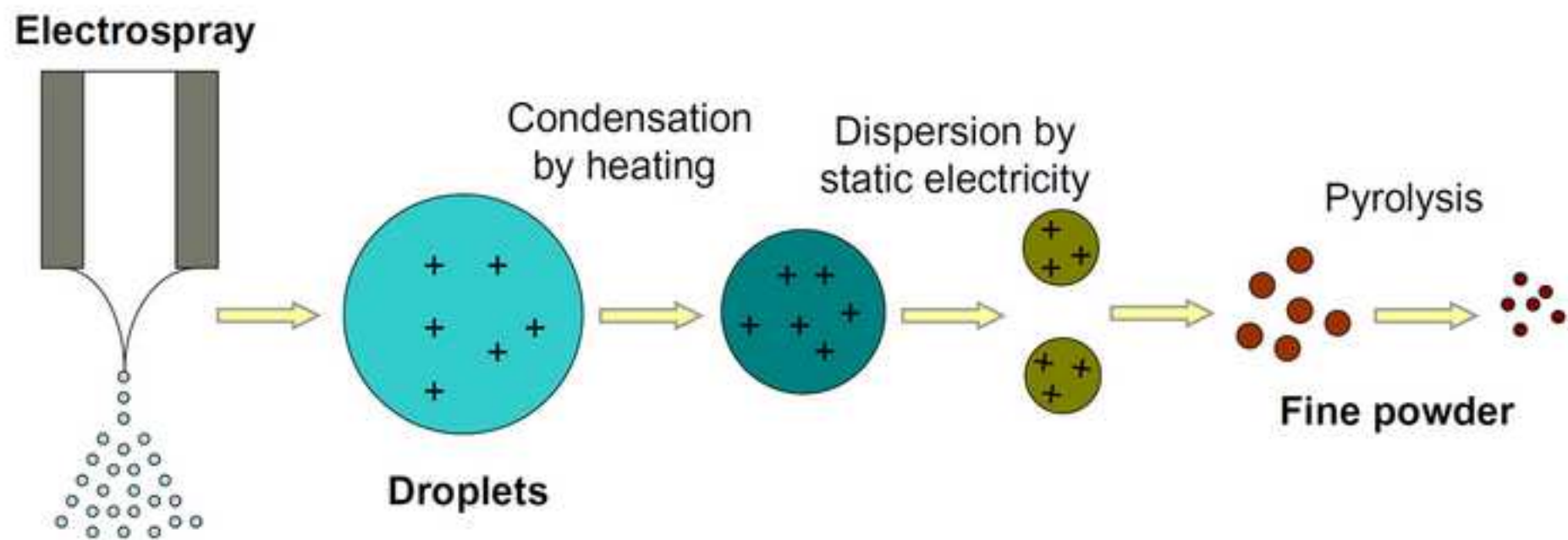


Figure2

[Click here to download high resolution image](#)

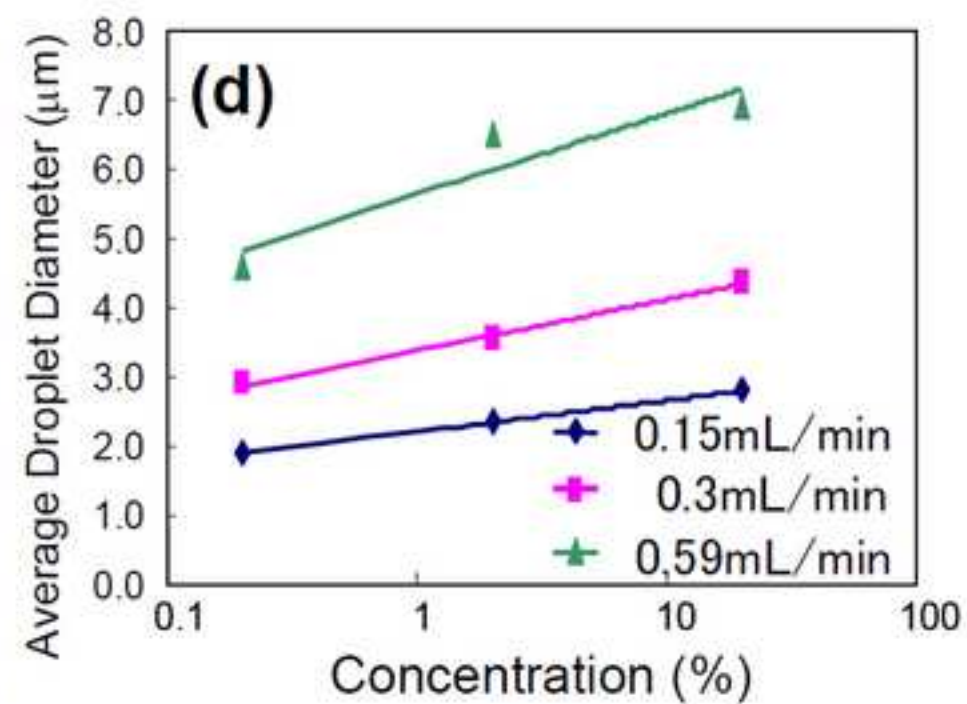
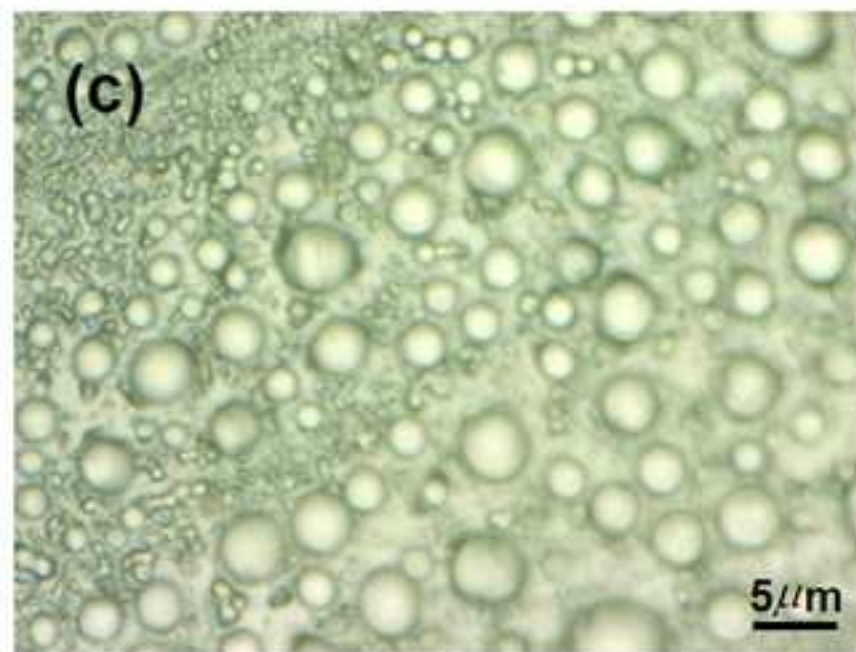
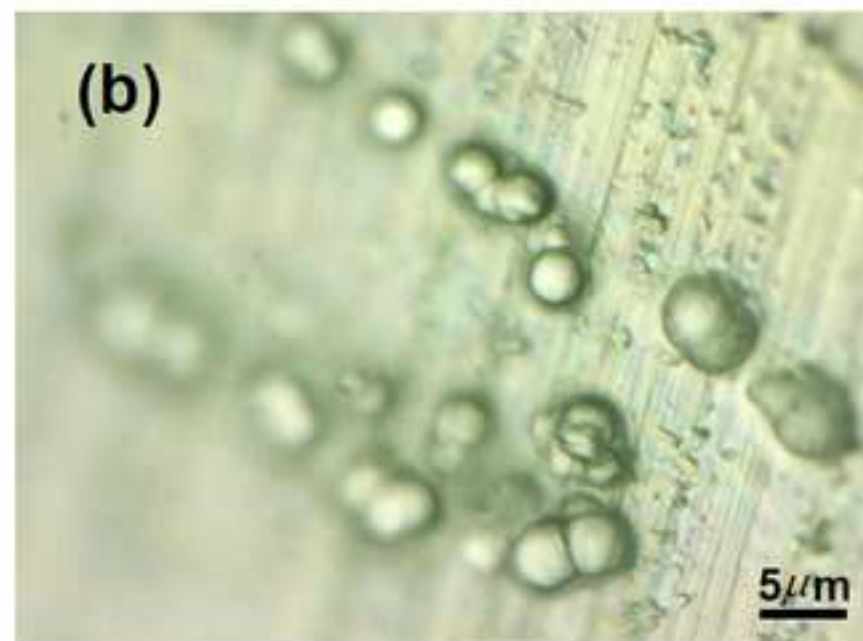
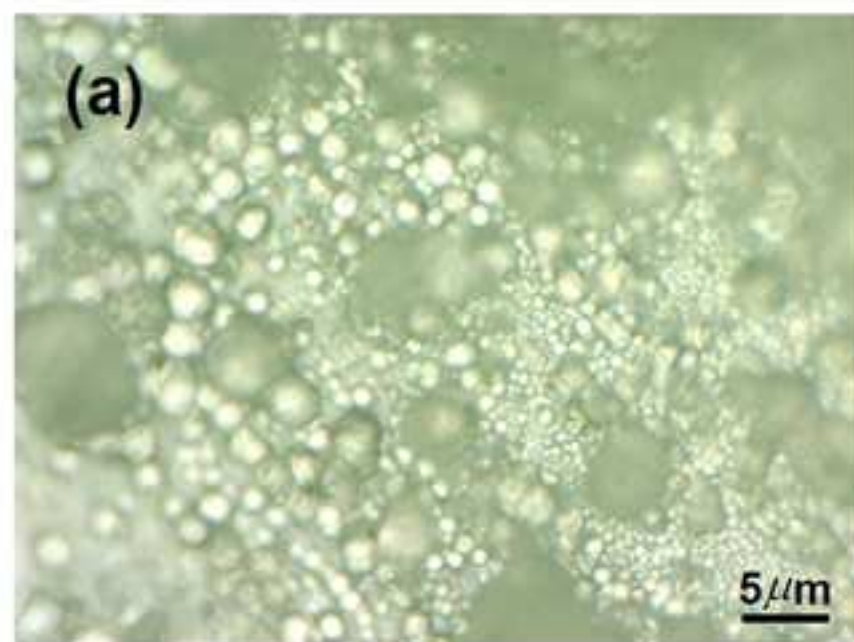




Figure3

[Click here to download high resolution image](#)

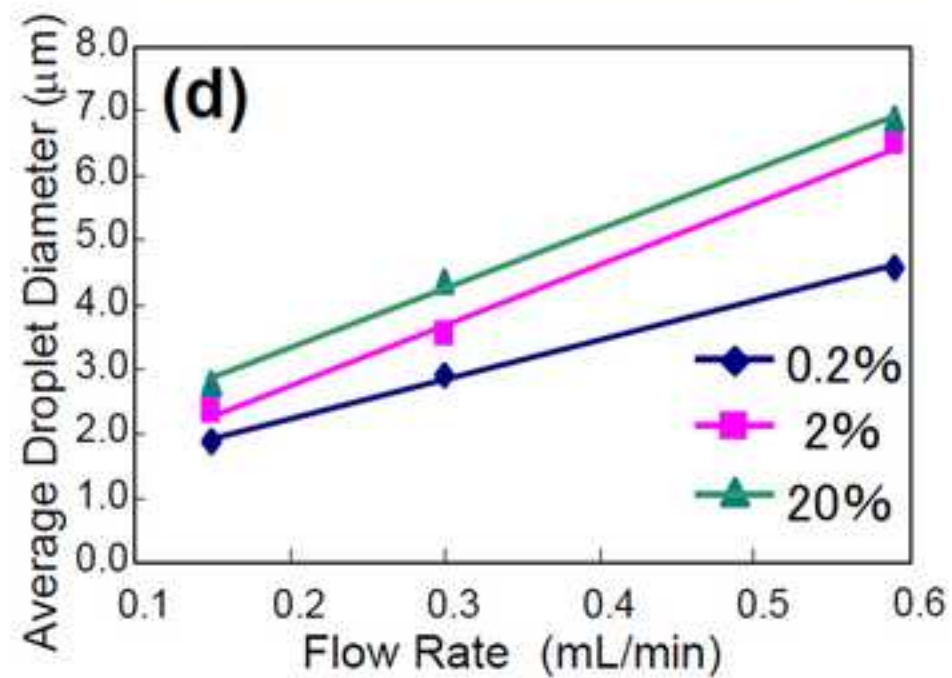
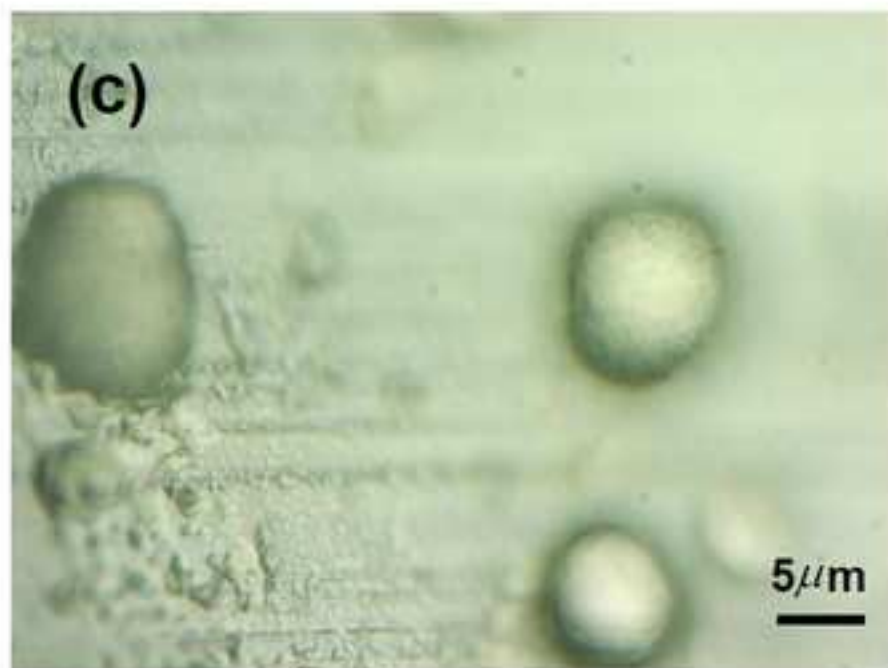
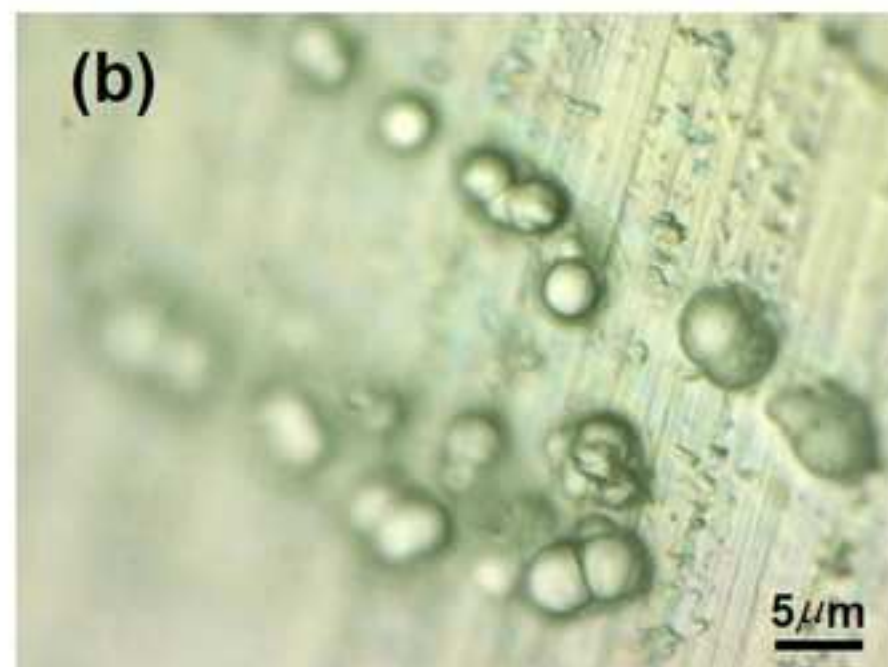
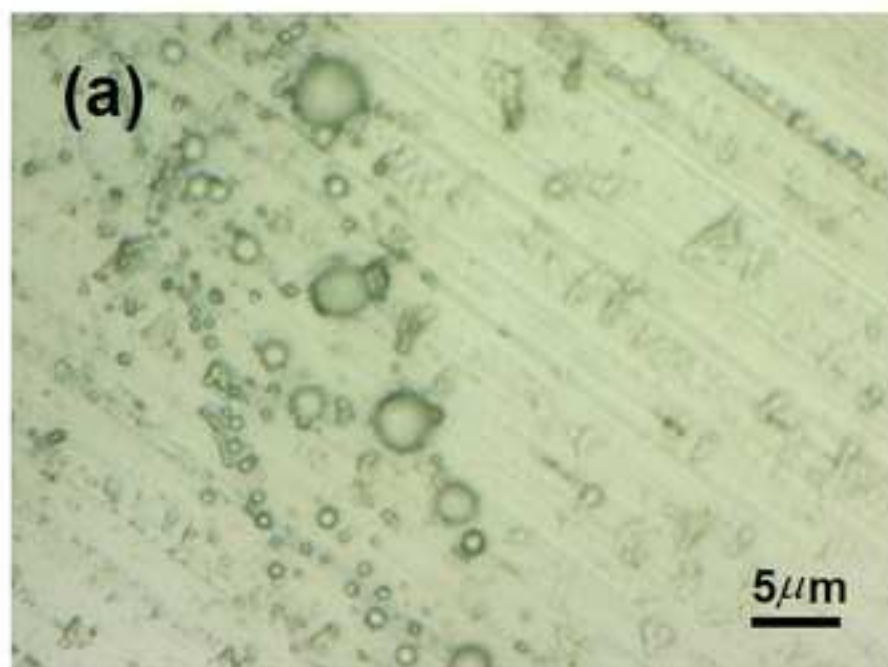




Figure4

[Click here to download high resolution image](#)

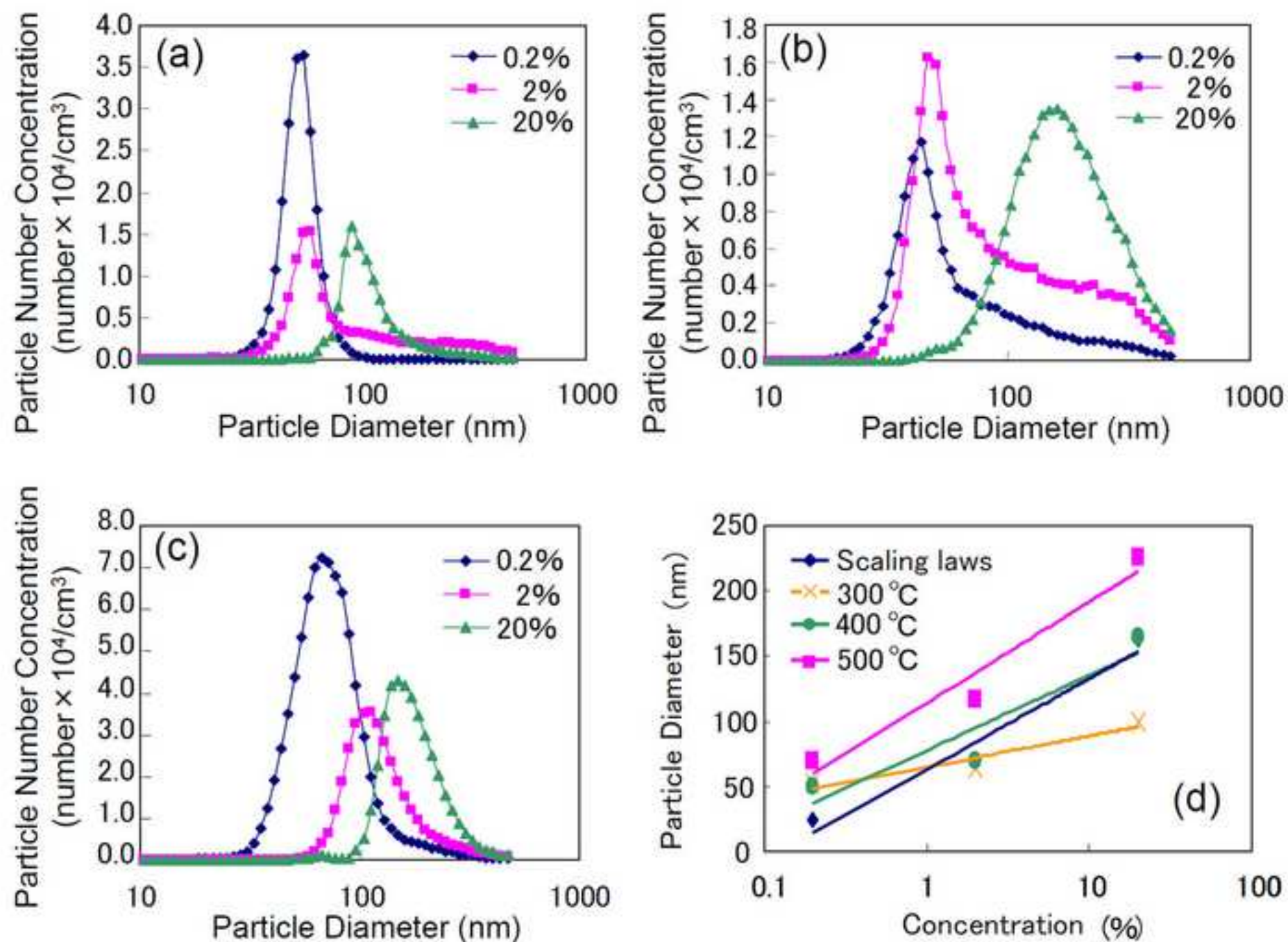


Figure5

[Click here to download high resolution image](#)

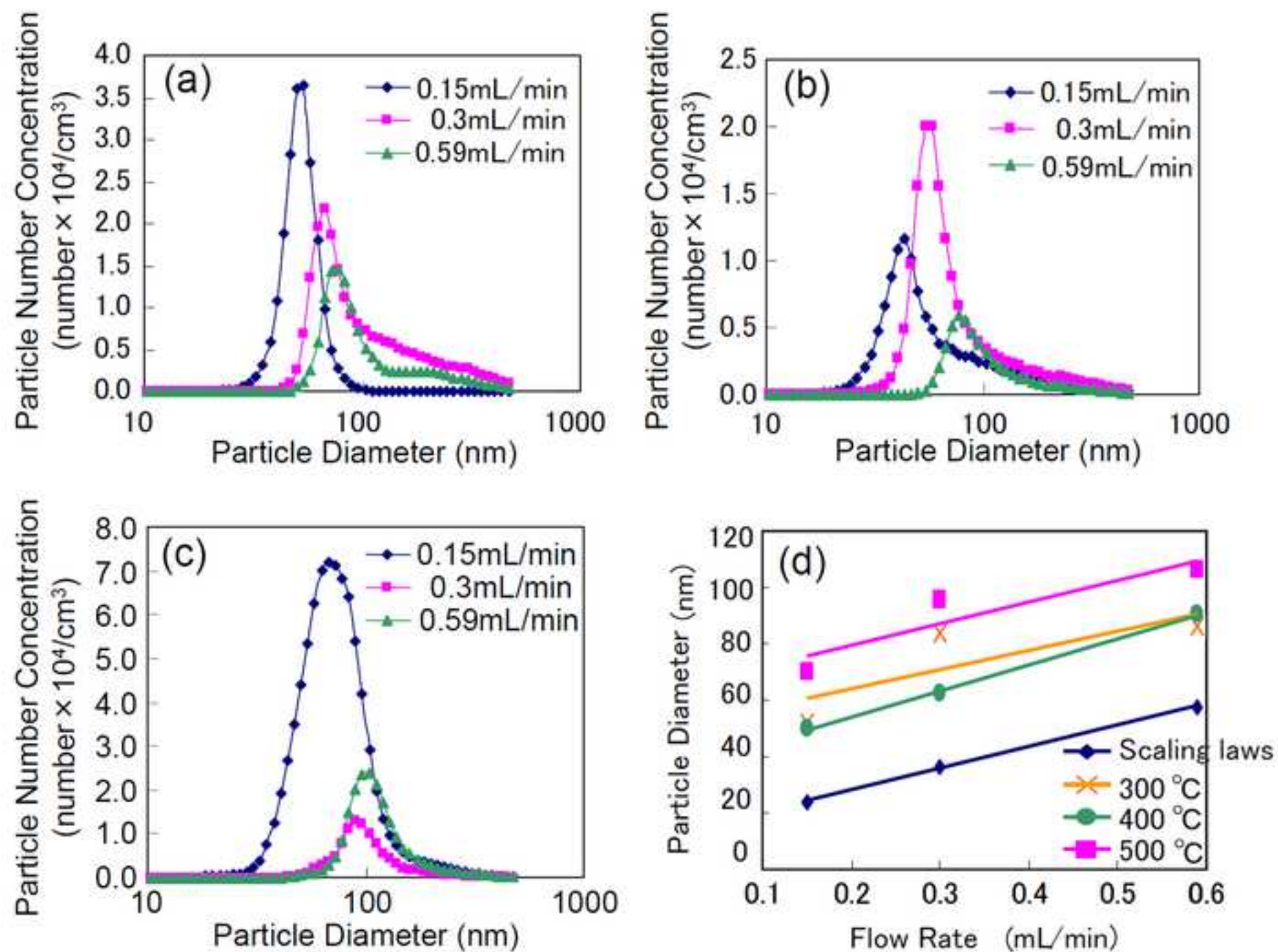


Figure6  
[Click here to download high resolution image](#)

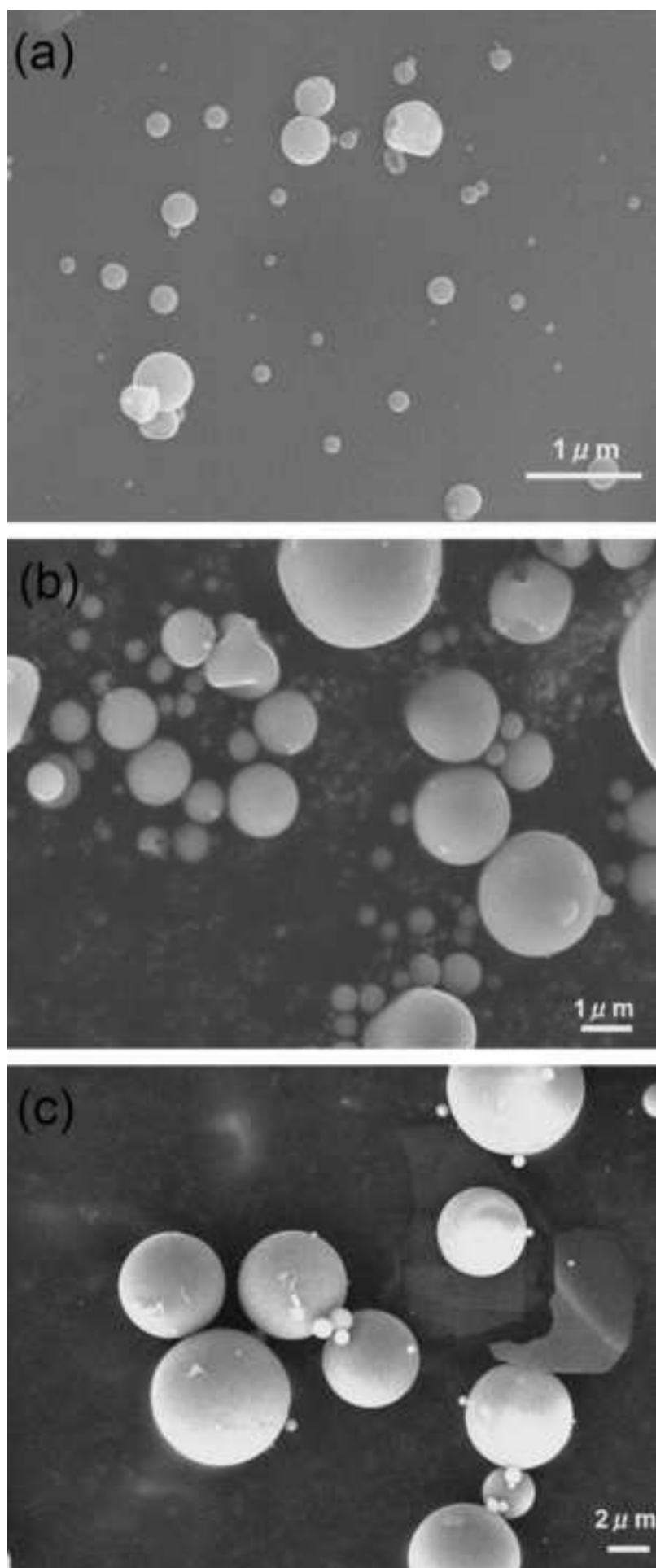




Figure7

[Click here to download high resolution image](#)

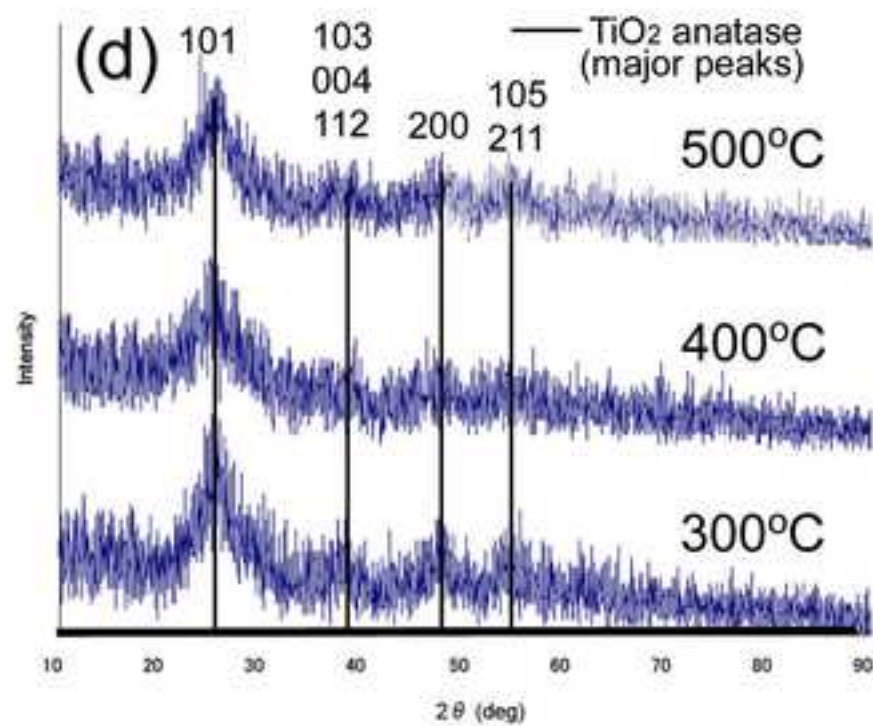
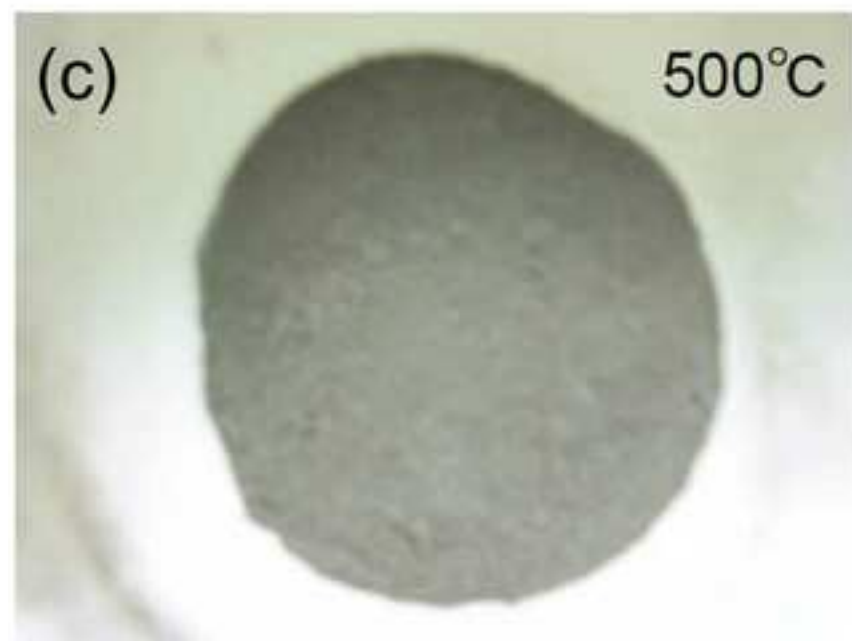
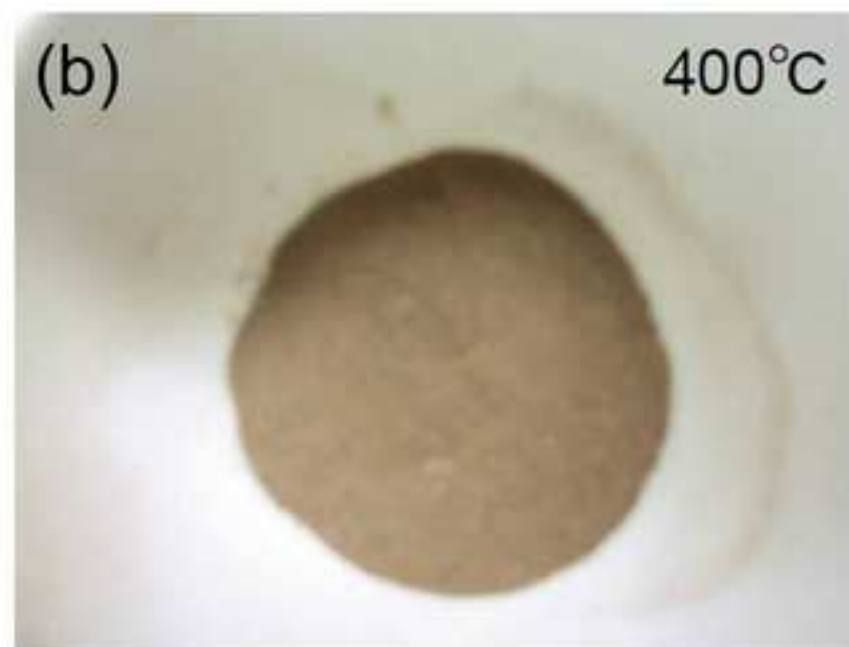
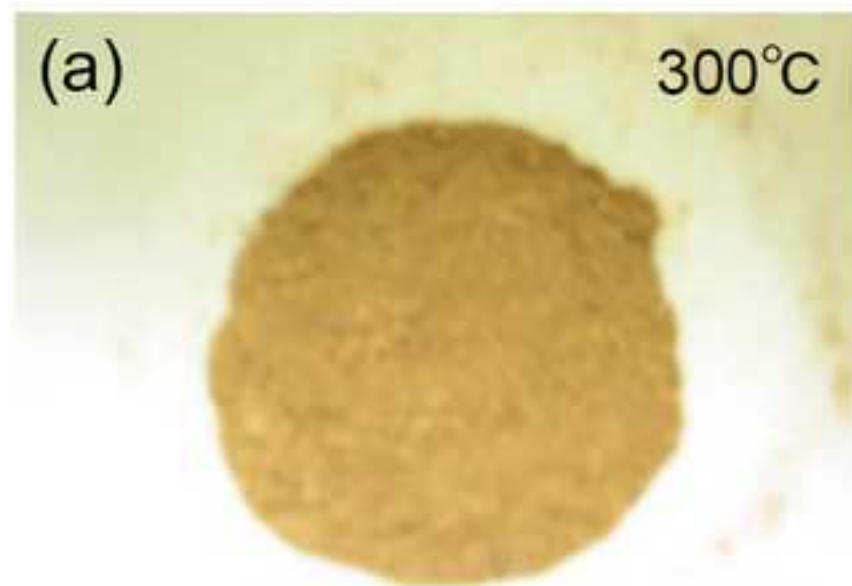


Figure8

[Click here to download high resolution image](#)

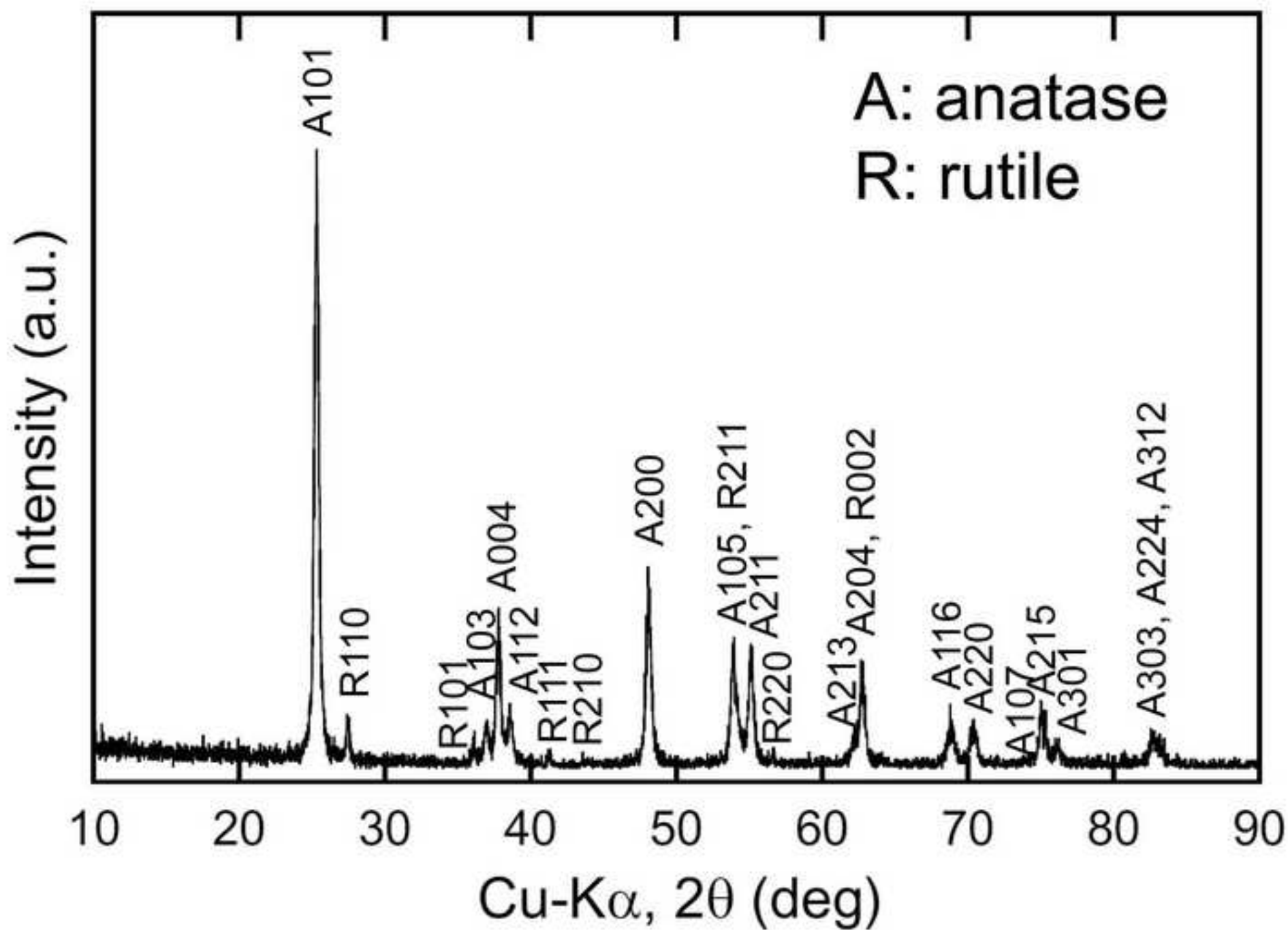
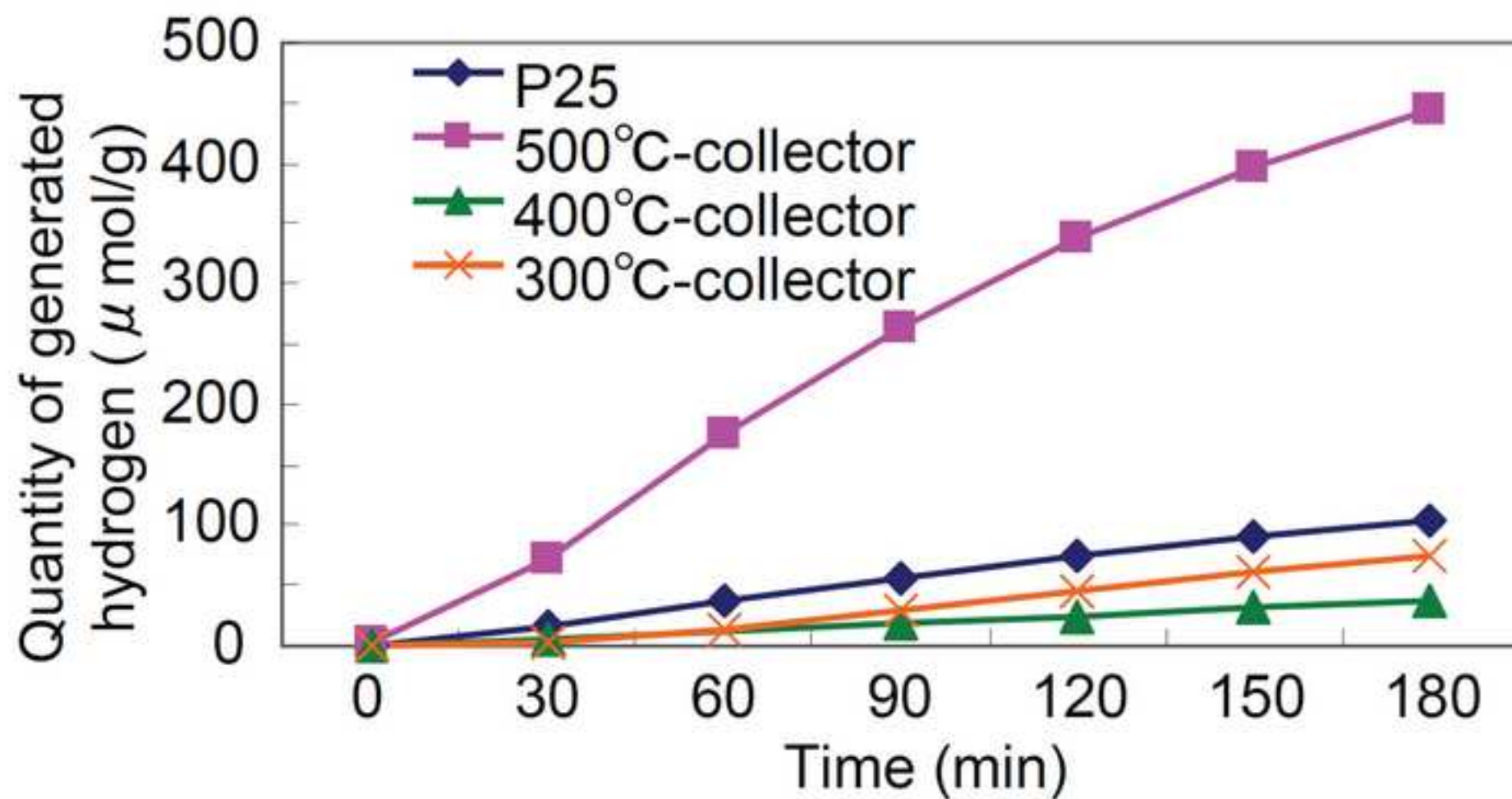


Figure9

[Click here to download high resolution image](#)



## Supplementary Material

[Click here to download Supplementary Material: FigureS1.jpg](#)